High Dynamic Range Image Reconstruction using Multiple Images

Jongseong Choi, Young-seok Han and Moon Gi Kang

Institute of TMS information technology,

Yonsei University

134, Shinchon-Dong, Seodaemoon-Ku, Seoul 120-749, Korea

Tel:+82-2-2123-4863 Fax:+82-2-312-4584

E-mail : mkang@yonsei.ac.kr

Abstract: The dynamic range of image sensors is limited due to the capacitance of photodiode and the nonlinearity of the system response function. In this paper, the high dynamic range image reconstruction algorithm using multiple images is proposed. The proposed algorithm simultaneously enhances dynamic range and estimates the imaging system's response function. The image acquisition process including limited dynamic range is modelled. With the observation model, the linear least squares estimates the response function of the imaging system as well as the single high dynamic range image are obtained.

1. Introduction

Digital images become increasingly important in many fields, such as medical tomography, industrial monitoring system, surveillance system, computer vision system, scientific research applications, broadcasting system, consumer appliances, etc. Digital images are two dimensional arrays of digitized brightness value of the natural scene. But, these pixel values are not true measurements of relative radiance in the scene. The human visual system exhibits an enormous optical dynamic range from the scotopic threshold to the glare limit, as it can adapt to an extremely high level of light intensity. This capability is also required in numerous digital imaging applications. Imaging sensors, however, have a narrow limited dynamic range comparing with the human visual system and the captured image of a scene has limited brightness range. Low dynamic range is one of the main problems when an image is acquired from image sensors[1]. When capturing a scene with a very wide intensity range of light that exceeds the dynamic range of an imaging sensor, it is inevitable to lose detail in either dark areas, bright areas or both. By controlling either exposure time, aperture size or both, we can choose the luminance level of the captured image. For example, with increased exposure time or aperture size, we can obtain a better representation of dark areas at the cost of losing information in bright areas. However, adjusting the exposure time or aperture size does not help to represent both low- and high-light areas of the scene with high dynamic range. Details will be definitely lost, and varying the exposure time just allows some control over where the loss occurs. To enhance the dynamic range, the new architectures of image sensors have been proposed[2]-[7], and the algorithmic techniques to increase the dynamic range of an image using differently exposed multiple frames of the same scene have been researched [8]-[10].

In this paper, the image acquisition process including limited dynamic range is modelled. With the image acquisition model, the linear least squares estimates the response function of the imaging system and reconstructs the single high dynamic range from multiple images, simultaneously. In the reconstruction process, the response function of the imaging system is updated in every iteration step. Experimental results indicate that the proposed algorithm outperforms the conventional approaches with assumption that the response function of the imaging system is known.

The rest of this paper is organized as follows. The proposed image reconstruction algorithm is introduced in Section 2. In Section 3, experimental results are presented and conclusions follow in Section 4.

2. Proposed high dynamic range image reconstruction algorithm

The proposed algorithm estimates the response function of imaging system and reconstructs the high dynamic range image, simultaneously. For this purpose, the image acquisition process including limited dynamic range of image sensor and quantization process is modelled. With the image acquisition model, the response function of the imaging system and the single high dynamic range image are estimated with the linear least squares estimates and Gauss-Seidel iteration method.

2.1 The image acquisition model

In order to model the image acquisition process, we use the reciprocity which means that the exposure is defined as the product of the irradiance r at the surface of image sensors and exposure time Δt[11]. In addition, Hurter-Driffield curve is used as the response function of an imaging system which curve is a graph of the optical density of the imaging sensor against the logarithm of the exposure $r\Delta t$. The typical shape of Hurter-Driffield curve is shown in Fig. 1.

Assume that there are N pictures of a static scene with different exposure times Δt_k where $k = 1, \ldots, N$. The k-th observed frame Y_k is given by

$$Y_k(i,j) = f(X(i,j)\Delta t_k) + N_k(i,j) \qquad (1)$$

where $f(\cdot)$ is a nonlinear function which is the composition of the characteristic function of the image capture device and the quantization process and N_k is the quantization noise. Generally, the function f for an 8-bit system has the form as

$$f(z) = \begin{cases} 0 & for\ z \in [0, I_0] \\ m & for\ z \in (I_{m-1}, I_m], \\ 255 & for\ z \in (I_{254}, \infty) \end{cases} \qquad (2)$$
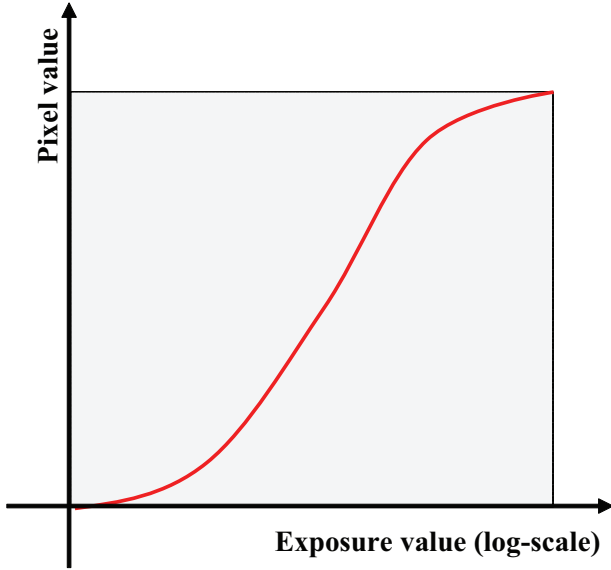
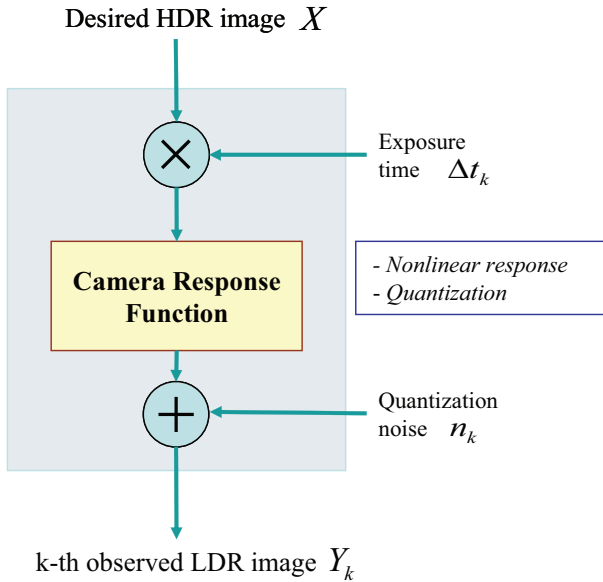Figure 1. Typical shape of Hurter-Driffield curve.

Figure 2. The block-diagram of the image acquisition model.

where I_{m-1} is the lower bound and I_m is the upper bound of the m-th quantization interval. A block diagram for the observation model is illustrated in Fig. 2.

2.2 Reconstruction of the high dynamic range image

To reconstruct the high dynamic range image based on the proposed image acquisition model, the inverse function of $f(\cdot)$ is required. However, the inverse function $f^{-1}(\cdot)$ does not exist because is a many-to-one mapping due to the quantization process. Therefore, the reverse mapping function $g(\cdot)$ is defined as the function which maps the pixel intensity to the mid-level of the corresponding quantization interval, and used instead of $f^{-1}(\cdot)$.

With the definition of the reverse mapping function and Taylor series expansion, the image acquisition model can be
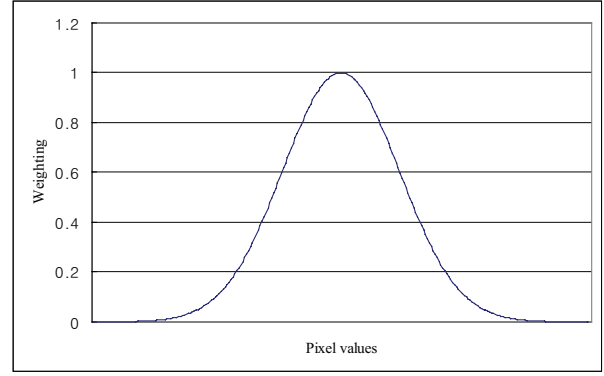

Figure 3. The Gaussian weighting function.

rewritten as

$$g(Y_k(i,j)) = X(i,j)\Delta t_k + N_k^T(i,j) \qquad (3)$$

where N_k^T is the total noise term including both quantization noise and reverse mapping error. The total noise N_k^T will be modelled as zero-mean independent Gaussian random variables with variances $\sigma_k^2(i,j)$. Accurately characterizing the variances $\sigma_k^2(i,j)$ would be extremely difficult, as it would require detailed knowledge of the specific image capture device being used. The total noise term can be expressed by

$$N_k^T(i,j) = g(Y_k(i,j)) - X(i,j)\Delta t_k. \qquad (4)$$

Because the reverse mapping function $g(\cdot)$ is unknown as well as the high dynamic range image X, the problem is formulated as simultaneous estimation of the reverse mapping function $g(\cdot)$ and reconstructs the high dynamic range image X that minimize the quadratic objective function given as

$$O = \sum_k \sum_i \sum_j w(Y_k(i,j))[g(Y_k(i,j)) - (X(i,j)\Delta t_k)]^2$$
$$(5)$$

where $w(\cdot)$ is the weighting function. Since the function is nonlinear and generally have a steep slope near minimum pixel value I_{min} and maximum pixel value I_{max}, the data will be fitted more poorly near these boundaries. A weighting function should be chosen such that the pixel values near $I_{mid} = (I_{min} + I_{max})/2$ are weighted more heavily than those near I_{min} and I_{max}. Therefore, the weighting function chosen in the proposed algorithm is a shifted Gaussian-like function formulated as

$$w(I) = \exp\left\{-\alpha\frac{(I - I_{mid})^2}{I_{mid}^2}\right\} \qquad (6)$$

where α is the constant that control the width of weighting function. This weighting function has the value 1 at I_{mid} and the value zero at I_{min} and I_{max} as shown in Fig. 3. This choice of the weighting function is reasonable considering the saturation near I_{min} and I_{max}.

Gauss-Seidel relaxation is used to determine the solution for both $g(\cdot)$ and X. Gauss-Seidel relaxation minimizes an objective function with respect to a single variable, and then

uses these values when minimizing with respect to subsequent variables. The quadratic objective function will be minimized with respect to $g(\cdot)$ and then minimized with respect to X. This constitutes one iteration process of the algorithm.

First, to reconstruct high dynamic range image X, Eq. (5) is minimized with respect to X, the partial derivative of Eq. (5) with respect to $X(a,b)$ is taken and set equal to zero as

$$\frac{\partial O}{\partial X(a,b)} = \sum_k \frac{2w(Y_k(a,b))[g(Y_k(a,b)) - X(a,b)\Delta t_k]}{\Delta t_k}$$
$$= 0. \qquad (7)$$

The reconstructed high dynamic range image X is

$$X(a,b) = \frac{\sum_k w(Y_k(a,b))g(Y_k(a,b))/\Delta t_k}{\sum_k w(Y_k(a,b))}. \qquad (8)$$

By Gauss-Seidel relaxation, the reverse mapping function g is estimated with the reconstructed X of the Eq. (8). Generally, estimation of g only requires recovering the finite number of values, since the values of the pixel brightness are finite. For example, the 256 values $g(z)$ for $z = 0, \cdots, 255$ are needed to be recovered for 8-bit system. Similarly, the minimization with respect to $g(z)$ is also calculated as

$$g(z) = \frac{\sum_{(k,i,j)\in I_z} w(z)[X(i,j)\Delta t_k]}{\sum_{(k,i,j)\in I_z} w(z)} \qquad (9)$$

where $I_z = \{(k,i,j)|Y_k(i,j) = z\}$ is the set of indices such that the pixel intensity z was observed for the low dynamic range images.

3. Experimental result

In order to demonstrate the performance of the algorithm, several experimental results are presented here. Figure 4 is the set of the low dynamic range images which are taken with different exposure times. As shown in Fig. 4, controlling the exposure time does not help to represent both low- and high-light areas For example, with increased exposure time, the details of dark region can be enhanced at the cost of losing information in bright region. Figure 5 is the reconstructed high dynamic range image by the proposed method. In order to display the result with conventional image format, the reconstructed image was compressed with a simple log scale mapping. As shown the Fig. 5, the proposed method significantly enhances the details in both dark region and bright region.

The reverse mapping function g is simultaneously estimated with the reconstruction of a single high dynamic range image. Figure 6 presents the estimated $g(\cdot)$ by the the conventional method (CM) and the proposed method. CM estimates the 256 values $g(z)$ for $z = 0, \ldots, 255$ for 8-bit system using singular value decomposition in advance. Compared with the result of CM, the estimated g by the proposed algorithm well maintains the typical form of the inverse Hurter-Driffield curve. Since g takes the role of mapping pixel values to high dynamic range radiance values, the fluctuation of g can cause the inversion of the local contrast of the reconstructed high
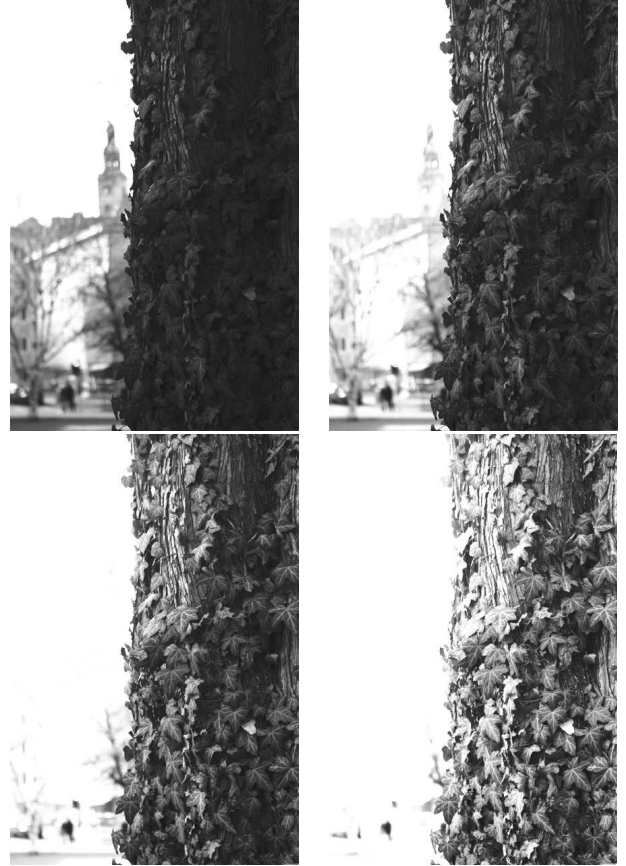

Figure 4. Four low dynamic range images.

dynamic range image. Since the reconstructed g of the proposed algorithm is smoother than the result of the CM, the proposed method reconstructs a more accurate high dynamic range image.

4. Conclusion

Since a high dynamic range image has more light intensity information than a low dynamic range image, it is very useful in the fields such as biometrics, medical imaging and astronomical imaging. Dynamic range enhancement based on signal processing approach has the advantage that it can be applied to the existing imaging devices in relatively low price as compared to the methods to manufacture the new architecture of image sensors.

We have proposed a signal processing based method for the reconstruction of a high dynamic range image from multiple low dynamic range frames with different exposures. The image degradation process including limited dynamic range is modelled and both the system response function and a single high dynamic range image are simultaneously obtained. The system response function is simultaneously estimated in every iteration step with the reconstruction of a single high dynamic range image. With the simulation results, it is shown that the proposed algorithm outperforms the the conventional approaches with respect to both objective and subjective criteria. Simulation results verify that the proposed algorithm
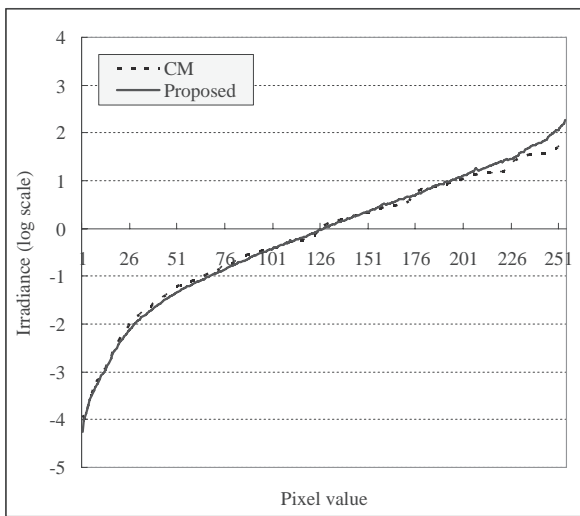
Figure 5. The reconstructed high dynamic range image.

Figure 6. The reconstructed reverse mapping function using the conventional and the proposed method.

estimates the reverse mapping function *g* without any prior knowledge about the system response function as well as a high dynamic range image.

Acknowledgements

References

[1] M. G. Kang. (2003) *SPIE Milestone Series Vol. MS177 Selected Papers on CCD and CMOS Imagers*. SPIE Press, Washington.

[2] Technical Report MS-CIS-93-96 (1993) Extended Intensity Range Imaging. Grasp Laboratory, Univ. of Pennsylvania

[3] K. Yamada, T. Nakada, and S. Yamamoto. (1994) Wide Dynamic Range Vision Sensor for Vehicles. *Proc. IEEE Conference on Vehicle Navigation and Information Systems Conference, 1994.*, August, pp. 405–408.

[4] V. Brajovic and T. Kande. (1996) A Sorting Image Sensor: An Example of Massively Parallel Intensity-to-time Processing for Low-latency Computational Sensors. *Proc. International Conference on Robotics and Automation, 1996.*, **2** September. pp. 1638–1643.

[5] R. A. Street. (1998) High dynamic range segmented pixel sensor array. *U. S. Patent 5789737*, August.

[6] S. k. Nayar and T. Mitsunaga. (2000) High dynamic range imaging: spatially varying pixel exposures. *Proc. IEEE Conference on Computer Vision and Pattern Recognition, 2000.*, **1**, June, pp. 472–479.

[7] M. Aggarwal, N. Ahuja. (2001) Split aperture imaging for high dynamic range. *Proc. IEEE International Conference on Computer Vision, 2001. (ICCV 2001.)*, **2**, July, pp. 10–17.

[8] C. Kolb, D. Mitchell, P. Hanrahan. (1995) A Realistic Camera Model for Computer Graphics. *Computer Graphics, Proceedings of SIGGRAPH '95*, pp. 317–324.

[9] P. E. Debevec and J. Malik (1997) Recovering High Dynamic Range Radiance Maps from Photographs. *SIGGRAPH 97 Conference proceedings*, 3-8 August, pp. 369–378.

[10] M. A. Robertson, S. Borman, and R. L. Stevenson. (1999) Dynamic Range Improvement through Multiple Exposures. *Proc. IEEE International Conference on Image Processing, 1999. (ICIP 99.)*, **3**, October, pp. 159–163.

[11] T. Tani (1995) *Photography Sensitivity : Theory and Mechanisms*, Oxford University Press.